Scientific Research Publishing

Energy and Power Engineering, 2026, 18(11), 758-776
https://www.scirp.org/journal/epe
ISSN Online: 1947-3818
ISSN Print: 1949-243X

Modeling and Analysis of Electrical Protection Systems: The Case of ZIZ Energie Mongo's H61 Substations in the Sahelian Zone of Guéra (Chad) during the Rainy Season

Yacoub Nassian Nimir[1,2], Haroun Abba Laban[1], Moussa Ahmat[2,3], Mahamat Wadi[1]

[1]Faculty of Engineering Sciences and Techniques, Polytechnic University of Mongo, Ndjamena, Chad
[2]National Advanced School of Engineering of Maroua, University of Maroua, Maroua, Cameroon
[3]Higher Teachers' Training School of Bongor, Bongor, Chad
Email: yacoubnassiannimir@yahoo.fr

How to cite this paper: Nimir, Y.N., Laban, H.A., Ahmat, M. and Wadi, M. (2026) Modeling and Analysis of Electrical Protection Systems: The Case of ZIZ Energie Mongo's H61 Substations in the Sahelian Zone of Guéra (Chad) during the Rainy Season. *Energy and Power Engineering*, **18**, 758-776.
https://doi.org/10.4236/epe.2026.1811035

Received: September 15, 2026
Accepted: November 2, 2026
Published: November 5, 2026

Copyright © 2026 by author(s) and Scientific Research Publishing Inc.
This work is licensed under the Creative Commons Attribution International License (CC BY 4.0).
http://creativecommons.org/licenses/by/4.0/

Open Access

Abstract

Mongo, the capital of the Guéra province, is located within the central Chadian massif, in the heart of the Sahel-Sudan belt. It lies between 12˚10'58"N and 18˚41'05"E, in a strategic climatic zone subject to the seasonal oscillations of the Intertropical Convergence Zone and, consequently, to climatic constraints. The rainy season extends from May/June to October, with annual precipitation ranging from 300 to 800 mm; the peak of the season occurs in July and August. In this region, lightning-induced overvoltages pose the most severe challenges for H61 transformer substations due to high lightning activity and humidity. These climatic factors compromise grid stability and expose overhead distribution substations to significant risks of insulation breakdown caused by atmospheric overvoltages. This study focuses on modeling a protection system for H61 overhead substations operated by the local electricity utility (ZIZ Énergie) in Mongo a Sahelian zone specifically during the rainy season. A key aspect of the analysis is examining the behavior of the H61 transformer both with and without ZnO (zinc oxide) surge arresters. The results demonstrate that, in the absence of protection (*i.e.*, without ZnO surge arresters), lightning strikes cause severe damage to the H61 transformer, impairing its operation and potentially rendering it inoperable. Integrating surge arresters and ensuring they are positioned as close as possible to the transformer provides effective and adequate protection. Furthermore, this research provides a valuable decision-support tool for researchers and experts in the field of electrical protection. MATLAB/Simulink is used for this purpose.

Keywords

MATLAB/Simulink, Lightning, ZnO Surge Arrester, H61 Substation, Distribution Network, ZIZ Energie de Mongo, Rainy Season, Sahelian Zone, Keraunic Level, Grounding

1. Introduction

Electrical substations can be subjected to atmospheric overvoltages, particularly during the rainy season. These overvoltages cause significant damage, impairing the proper functioning of distribution substations. Consequently, a highly efficient and reliable protection system is required—a need that has historically presented real challenges. The objective of this study is to utilize zinc oxide (ZnO) surge arresters to optimize the protection system for H61 substations [1] under the climatic conditions of the Sahelian zone, specifically in the Guéra Province.

Lightning strikes can be direct hitting a conductor or indirect striking a pylon or the overhead ground wire [2]. This study focuses on a direct lightning strike on the 160 kVA distribution substation at the Mongo power plant. The system is modeled using a complete three-phase schematic that includes all components connected to the substation. Simulations were performed in the MATLAB/Simulink environment, comparing scenarios with and without surge arresters installed upstream of the 15 kV/400V transformer.

Simulations involving the injection of a standardized 1.2/50 μs transient voltage impulse (IEC 60099-4) and a standardized 8/20 μs discharge current wave (IEC 60099-4) demonstrate that, without surge arresters, the lightning impulse significantly exceeds the transformer's 95 kV Basic Insulation Level (BIL), inevitably leading to its destruction. Conversely, with ZnO surge arresters, the voltage wave is effectively clamped to a safe residual voltage level [3].

Previous research has addressed these critical issues regarding electrical grid protection. Aoues *et al.* (2014) focus on optimizing protection within a specific medium-voltage (MV) network [4], while Safia and Lila (2014) investigate transformer protection against lightning-induced overvoltages, proposing practical methods that nonetheless require validation under real-world conditions [5]. Bedoui and Bayadi (2007) demonstrate the effectiveness of ZnO surge arresters in mitigating overvoltages at transformer substations but omit the costs associated with their implementation [1]. Mohamed and Faiz (2017) evaluate a protection system on the Sonelgaz grid, identifying vulnerabilities and suggesting improvements. Sadia and Amel (2014) propose modernizing autotransformer protection systems by incorporating modern technologies, although their study remains theoretical [6]. Mohamed (2010) analyzes protection in MV networks, questioning existing practices without offering immediate practical applicability [7]. None of these studies adequately address the specific case of the Guéra province in Chad.

Existing literature consistently highlights lightning as a major disruptive phe-

nomenon affecting all power ranges and voltage levels; it is the primary source of atmospheric overvoltages. However, studies conducted in temperate climates fail to account for the extreme variations in soil resistivity and keraunic levels characteristic of the Sahelian belt during the rainy season. Consequently, this research focuses on studying and modeling the protection system for 160 kVA H61 substations within the ZIZ Énergie 15 kV/400V network in the Sahelian zone of Mongo during the rainy season.

General Methodology

Section 2 outlines general information regarding surge arresters and the severe climatic stresses affecting H61 substations. Section 3 describes the study area in terms of its geographical and climatic characteristics. Section 4 presents the modeling of the protection system using MATLAB/Simulink. The results of statistical analyses concerning primary and secondary transformer voltages and currents—as well as protection distance, sensitivity, and overvoltages transmitted to the LV secondary side—are presented.

2. Materials and Methods

2.1. Study Area

The town of Mongo, the capital of the Guéra province in Chad, is located at coordinates 12˚10'58"N, 18˚41'05"E, within the central Chadian massif in the heart of the Sahel-Sudan belt. It is a strategic climatic zone subject to the seasonal oscillations of the Intertropical Convergence Zone and, consequently, to specific climatic stresses [8].

The rainy season is characterized by intense lightning activity resulting from the combination of the Sahel-Sudan climate and orographic relief. This heightens the area's exposure to atmospheric discharges and high humidity—factors that alter soil resistivity (and consequently grounding resistance), thereby increasing equipment vulnerability to atmospheric overvoltages and insulation failures.

2.2. H61 Architecture

Pole-mounted transformer substations (50 kVA, 100 kVA, 160 kVA) are installed on concrete poles. Pole quality and burial depth must comply with the standards required for Medium Voltage (MV) network installations [9].

Figure 1 shows a pole-mounted 160 kVA distribution substation belonging to ZIZ Energie in the town of Mongo.

Table 1 lists the specifications of the 160 kVA distribution substation. The rated low-voltage (LV) is 400 V. The selected earthing system is the TT arrangement, in which the transformer neutral and the installation's exposed conductive parts are connected to separate earth electrodes.

Personnel protection is strictly ensured by Residual Current Devices (RCDs) designed to cut the power supply immediately upon the occurrence of a first in-

sulation fault. The Basic Insulation Level (BIL) is 95 kV (1.2/50 μs wave) in accordance with the IEC 60076-3 standard.



Figure 1. ZIZ Energie 160 kVA distribution substation in mongo.

HRC fuse cutouts are located upstream; the step-down transformer (15 kV/400V), the main low-voltage circuit breaker, and the MV surge arresters crucially positioned are located at the point where the overhead line arrives, immediately before the transformer.

Table 1. The specifications of this substation are as follows.

160 kVA transformer			
Parameters	Symbols	Values	Normative references
Rated power	S_n	160 kVA	
LV rated voltage	U_n	400 V	
LV rated current	I_n	230.9 A	
Short-circuit voltage	U_{cc}	4%	CEI 60076
Prospective short-circuit current	$I_{cc}BT$	5.7 kA	
Connection type	$Dyn11$		CEI 60076
LV neutral earthing system	TT		CEI 60364/NF C 15-100
Neutral earthing resistor	R_B	≤15 Ω	Distribution Guide
Impulse withstand voltage level	BIL	95 kV (wave 1.2/50 μs)	CEI 60076-3

2.3. Lightning

Lightning is a violent electrical discharge of atmospheric origin that occurs between a cloud and the ground, taking the form of one or more strokes. This phenomenon is accompanied by a brilliant flash of light and a loud noise (thunder). Inside the cloud, violent updrafts and downdrafts cause collisions between water

molecules. These collisions generate positive charges that accumulate at the top of the cloud and negative charges that accumulate at its base. The separation of charges within the storm cloud creates an intense electric field in the space between the cloud and the ground. This results in electrical arcs: lightning [10].



Figure 2. Atmospheric lightning strike [11].

Figure 2 shows an image of lightning in the Sahel region during the rainy season.

2.4. Modeling of Electrical System Components

2.4.1. IEEE Surge Arrester Model [12]

Several research studies on zinc oxide (ZnO) surge arresters have focused solely on protection system analysis. Our study focuses on modeling and simulating the system incorporating the surge arrester (IEEE WG 3.4.11). The metal-oxide surge arrester exhibits a highly non-linear current-voltage (I-V) characteristic, modeled by the empirical equation:

$$I = k \cdot V^{\alpha} \tag{1}$$

With: $V = C \cdot I^{\frac{1}{\alpha}}$

The various variables in the equation are defined as follows:

V: Instantaneous voltage across the surge arrester (V).

I: Discharge current flowing through the device (A).

k or C: Geometric constants depending on the dimensions of the ZnO disc.

α: Non-linearity coefficient (or steepness) ranging from $3 < \alpha < 6$ for silicon carbide-based varistors and from $30 < \alpha < 50$ for ZnO-based varistors. This value accounts for the ultra-fast transition from insulator to conductor.

The voltage-current characteristic $V = f(I)$ of a ZnO varistor is illustrated by the curve in **Figure 3**. It is plotted on a semi-logarithmic scale (representing the overall physical characteristic), highlighting the highly non-linear behavior of the semiconductor material, which is structured around three operating regions: the leakage region, the clamping region, and the high-conduction region.

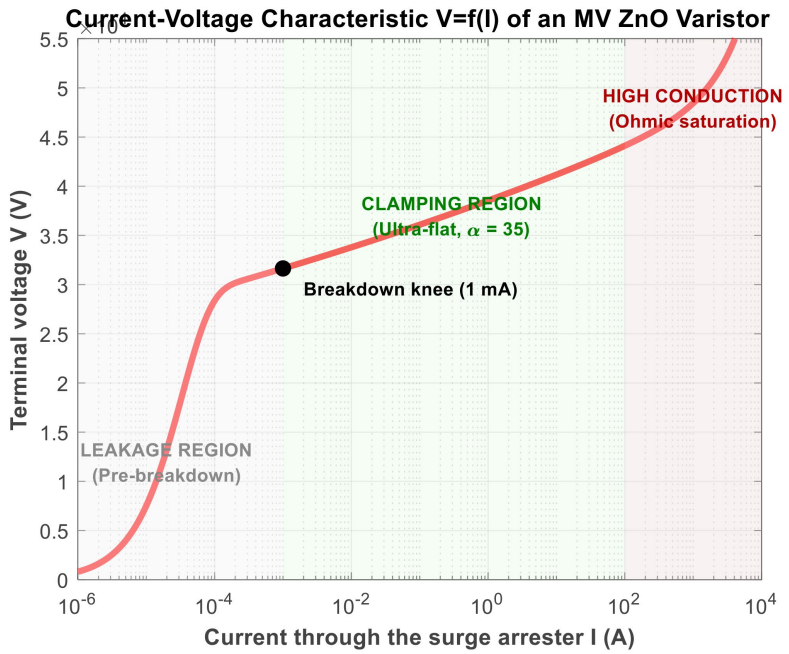


Figure 3. Voltage-current characteristic curve.

Analysis of data regarding the characteristics of metal-oxide surge arresters indicates that these devices also exhibit dynamic characteristics which are crucial when analyzing lightning or other fast-front surges and that this model is unsuitable for such conditions [13]. To account for frequency, a model is illustrated in **Figure 4**:

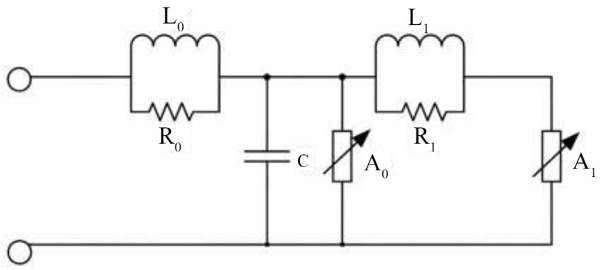


Figure 4. Modèle de IEEE [14].

Figure 4 shows the non-linear current-voltage characteristic model of the surge arrester. It features two non-linear sections separated by an R-L filter; for slow-rising stresses, the impedance of the R-L filters is extremely low, and consequently, the model's resistors are effectively connected in parallel. However, for very fast-rising waves, the impedance of the R-L filters increases; as a result, the R-L filters force high-frequency currents to flow primarily through the section designated as A_0 rather than the section designated as A_1. The model parameters are determined following the procedure outlined in the reference (IEEE WG. 3.4.11). An initial estimate of the circuit parameters is made using the following equations:

Inductance (coil) equations:

Magnetic behavior during the rapid rise of the current is represented by L_1:

$$L_1 = 15 \cdot \frac{d}{A} \tag{2}$$

The inductance of the wires and external physical connections is represented by L_0:

$$L_0 = 0.2 \cdot \frac{d}{A} \tag{3}$$

Resistor equations:

The internal high-frequency filter is stabilized by R_1:

$$R_1 = 65 \cdot \frac{d}{A} \tag{4}$$

R_0 helps adjust the transient response:

$$R_0 = 100 \cdot \frac{d}{A} \tag{5}$$

Equations for the capacitor (ZnO parasitic capacitance):

C represents the capacitive effect of the varistor in normal mode, in the absence of overvoltage:

$$C = \varepsilon_r \cdot \varepsilon_0 \cdot \frac{d}{A} \tag{6}$$

Non-linear elements V_{A0} and V_{A1}:

Their voltage-current (V-I) characteristics are not simple fixed values, but behavioral curves calculated proportionally based on our graph:

The internal varistor V_{A0} is set to follow the curve defined by the equation:

$$V_{A0} = 0.95 \cdot V_{ref} \tag{7}$$

The internal varistor V_{A1} is adjusted so that

$$V_{A1} = 1.05 \cdot V_{ref} \tag{8}$$

The parameters are defined as follows:

d: total length of the metal-oxide surge arrester (in meters).

A: number of parallel columns of metal-oxide surge arresters.

L_0: inductance associated with the magnetic field in the immediate vicinity of the surge arresters.

R_0: resistance used to stabilize numerical integration.

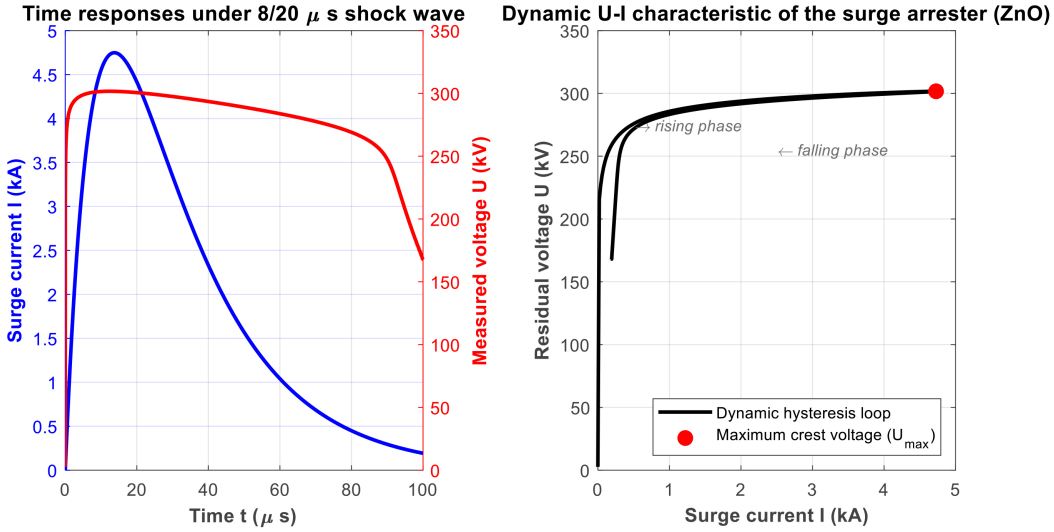
C: total capacitance of the surge arrester.

The elements A_0 and A_1 can be modeled in MATLAB/Simulink using exponential equations estimated from voltage-current data points.

These formulas provide a good starting point for selecting the optimal parameter values for the equivalent circuit. It should be noted that the model is highly sensitive to variations in L_1, whereas the other parameters have only a minimal influence. Figure 5 illustrates the dynamic behavior of ZnO surge arresters.

The curves in Figure 5 illustrate the effectiveness of the zinc oxide (ZnO)-based surge arrester during a lightning-type electrical surge (standard 8/20 μs wave-

form). Figure 5(a)—the time-domain plot—demonstrates that the component reacts immediately, clamping the voltage to a safe level (300 kV) despite the injection of a massive current pulse reaching nearly 5 kA. On the right, the V-I curve forms a closed loop (hysteresis); this highlights the surge arrester's highly dynamic behavior, showing that the voltage required to conduct current remains higher during the rapid rise phase of the lightning surge than during its slower decay phase.



(a) (b)

Figure 5. Dynamic behavior of the ZnO surge arrester.

2.4.2. Modeling the Protection System in MATLAB/Simulink

The key blocks of the Simulink diagram are described in this section.

1) Configuration of power blocks

The 15 kV source models the medium-voltage (15 kV) distribution network. The Pi-model line represents the power line impedance (distributed R, L, and C parameters) and models the physical behavior of the cable or overhead line transporting energy to the substation. The 160 kVA, 15 kV/400 V, Dyn11-connected three-phase transformer is the heart of the transformer substation [15].

Table 2 lists all the parameters entered into the MATLAB Simulink environment for all simulation scenarios.

Table 2. Numerical values entered into the MATLAB/Simulink model.

Settings		Numerical values
Line length		100 km
High-frequency parameters of the 160 kVA transformer		1nF
ZnO surge arrester parameters	Rated voltage	22×10^3 V
	Discharge current	10 kA, the most common standard value for H61 substations.

Continued

	Points on its V-I curve	$K_1 = 0.955$, $\alpha_1 = 30$ $K_2 = 1.0$, $\alpha_2 = 25$ $K_3 = 0.9915$, $\alpha_3 = 16.5$ $I_{ref} = 500$ A
Earth electrode resistance value	20 Ω	
Type of load connected to the secondary	Three-phase RLC load	
Numerical solver type	Ode23tb	

2) Configuration of the lightning generation block and surge arresters

The impulse source used to generate the surge is configured via the From *Workspace* block named *Foudre_Simulink*. This acts as an impulse current source (surge generator) that injects a transient waveform to simulate a direct or induced lightning strike on the network. The lightning scenario injected into the 15 kV medium-voltage network consists of a standardized 8/20 μs impulse current waveform. The characteristic parameters of this waveform are defined as follows:

Front time (T_1): 8 μs, representing the rapid rise time of the atmospheric discharge from 10% to 90% of its peak value.

Time to half-value (T_2): 20 μs, characterizing the duration required for the current to decay to half of its maximum amplitude.

This 8/20 μs waveform is injected to simulate the impact of a direct or induced lightning overvoltage near line H61. The simulations compare two distinct configurations to analyze stress attenuation:

The reference case (without surge arresters): To evaluate the transformer's intrinsic vulnerability and the exposure of low-voltage equipment to critical overvoltage transfers.

The protected case (with medium-voltage zinc oxide [ZnO] surge arresters): To quantify overvoltage clipping and the diversion of lightning current to ground through various earthing resistances (R_{earth} = 5, 25, 100 Ω), representing seasonal variations (such as the rainy season). The 8/20 μs impulse current is injected at the end of the overhead line directly connected to the upstream input terminals of the H61 substation.

The surge arrester units protect the transformer by clipping the lightning surge wave [16].

3) Modeling the digital protection logic chain

- **Control system block**

The upstream three-phase circuit breaker receives opening or closing commands issued by the actuator. The control signal, generated by the protection logic, enables the transformer to be instantly isolated from the MV grid in the event of a detected anomaly or fault. The downstream three-phase circuit breaker provides protection against overloads and short circuits, as well as disconnection of the Low Voltage (LV) section at the head of the load supply line.

- **Scaling of measured quantities (CTs and VTs)**

To adapt the high currents and voltages of the Mongo 15 kV grid to the input requirements of the protection logic chain, current and voltage instrument transformers are modeled.

For a 160 kVA three-phase transformer with a rated line-to-line voltage of 15 kV, the rated current on the medium-voltage side is calculated as follows:

$$I_{1n} = \frac{S_n}{U_n \cdot \sqrt{3}} = \frac{160\ \text{kVA}}{\sqrt{3} \cdot 15\ \text{kV}} = 6.16\ \text{A} \tag{9}$$

The current transformer must reduce this load current of approximately 6.16 A (including short-circuit currents) to a standard secondary current of 1 A or 5 A for the protection relay.

The voltage transformer must reduce the nominal phase voltage of the Mongo network. either $\frac{15\ \text{kV}}{\sqrt{3}} = 8.66\ \text{kV}$, to the standard measurement voltage of $\frac{100\ \text{V}}{\sqrt{3}}$ (ou $110/\sqrt{3}$ V). The nominal transformation ratio of the voltage transformer (TT) is therefore: $K_n = \frac{15000/\sqrt{3}}{100/\sqrt{3}} = 150$

A current transformer (CT) with a 50/5 A ratio ($m_{CT} = 10$) is selected. These scaling factors allow the inputs of the RMS calculation block to be calibrated.

4) Sizing of instrument transformers

Given a rated current of 6.16 A, a CT with the next highest standard primary rating is chosen to allow for a slight overload specifically 10 A (or a dual-ratio 10–20 A CT). The selected ratio will therefore be 10/5 A or 10/1 A.

During the rainy season, short-circuit currents on the overhead network can reach several hundred amperes.

As for the voltage transformer (VT), it must be specified for $\frac{15000}{\sqrt{3}}\text{V}$ at the primary level and $\frac{100}{\sqrt{3}}\text{V}$ at the secondary.

5) The RMS Block (signal measurement and processing)

The RMS (Root Mean Square) block calculates the RMS value of the measured signal to allow comparison with a fixed threshold.

The hysteresis relay compares the RMS value against a critical threshold (overcurrent or overvoltage). If the threshold is exceeded, it switches to 1.

The discrete delay block (Z^{-d}) handles logic processing, signal inversion, and the time delays essential for protection coordination (to prevent nuisance tripping).

The RS flip-flop (Set/Reset inputs) stores the fault status. As soon as the Set (S) input receives the trip command, output Q switches to 1 (opening command) and remains latched even if the fault clears temporarily until a Reset (R) signal is sent.

Figure 6 illustrates the overall Simulink model of ZIZ Énergie's 15 kV/400 V distribution network in Mongo, incorporating the power source, zinc oxide (ZnO) surge arresters, the H61 transformer, and the lightning injection system.

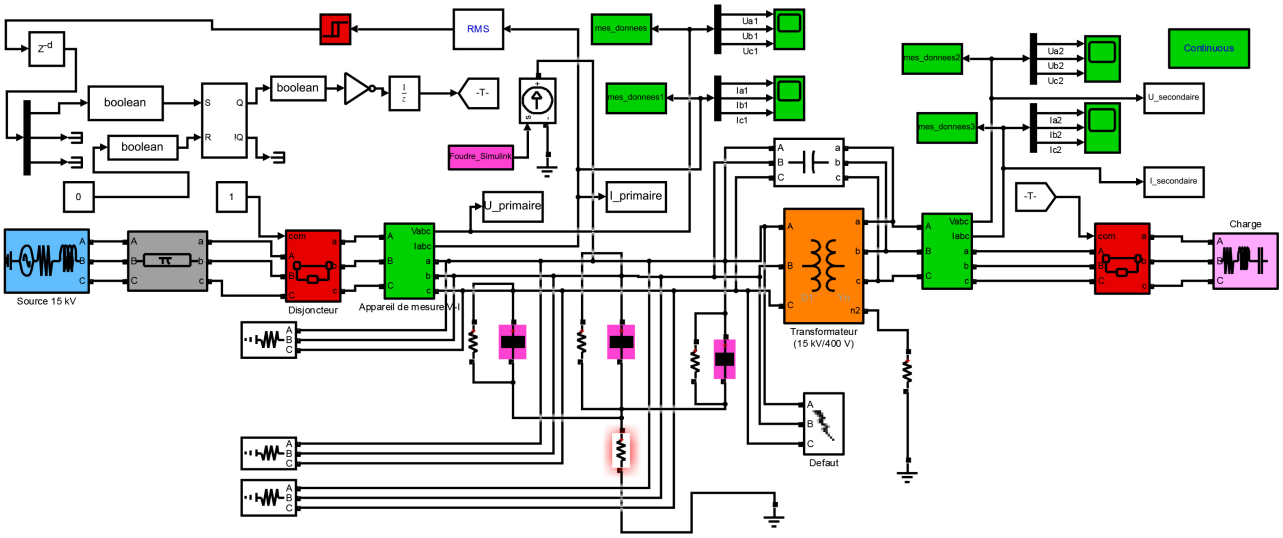


Figure 6. Model of the 160 kVA substation implemented in MATLAB/Simulink.

3. Results and Discussion

The MATLAB/Simulink environment is a valuable tool for analyzing lightning overvoltages in substations and conducting insulation coordination studies. A comprehensive system model allows for a detailed analysis of the complexities involved in substation overvoltage protection. The primary objective of this study is to evaluate voltage stresses within the substation in the absence of surge arresters, and subsequently to examine the scenario with surge arresters installed, specifically analyzing the impact of lightning current characteristics (amplitude, front time) and protection distance. The lightning surge is modeled as a current source with an 8/20 μs waveform striking a phase conductor of the line in question.

3.1. Stresses Experienced by the 160 kVA Substation

3.1.1. Transient Voltages at the Primary Side

Figure 7 shows the evolution of the overall instantaneous voltage of the 15 kV grid—specifically, the 50 Hz sinusoidal wave combined with the transient—on a millisecond timescale. The observation window, expanded from 20 to 35 ms, thus illustrates the impact of the transient on the 50 Hz sinusoidal waveform.

When the surge arresters activate, the "with surge arresters" curve shows the peak voltage stabilizing steadily around the grid peak plus the clipping effect, oscillating generally between 20 and 25 kV in this view. Figure 7 also illustrates the influence of the earth resistance (R_{earth} = 5 Ω, 25 Ω, 100 Ω) on the overall voltage envelope and shows that, in the transformer without surge arresters, the voltage rises to theoretically destructive levels exceeding 2500 kV.

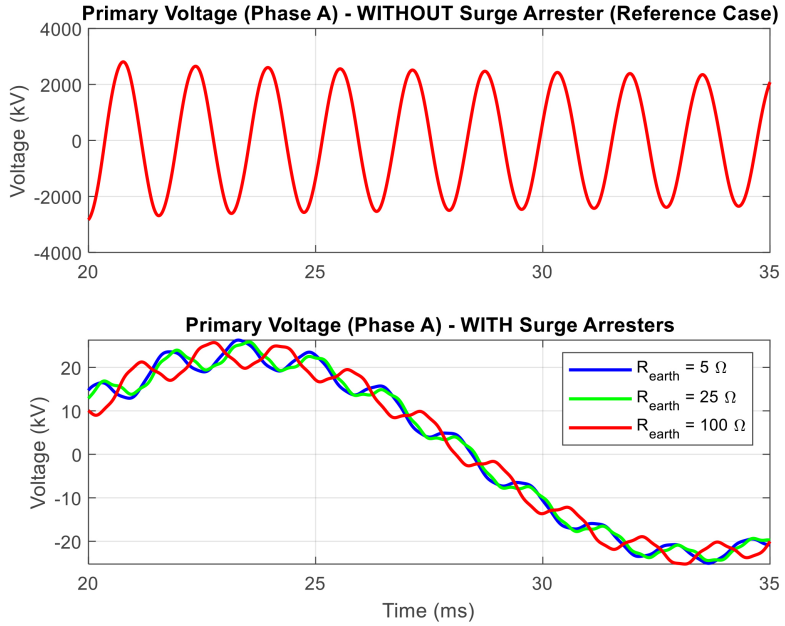


Figure 7. Waveform of the instantaneous primary voltage (Phase A) under sinusoidal and transient conditions.

3.1.2. Transient Currents on the Primary Side

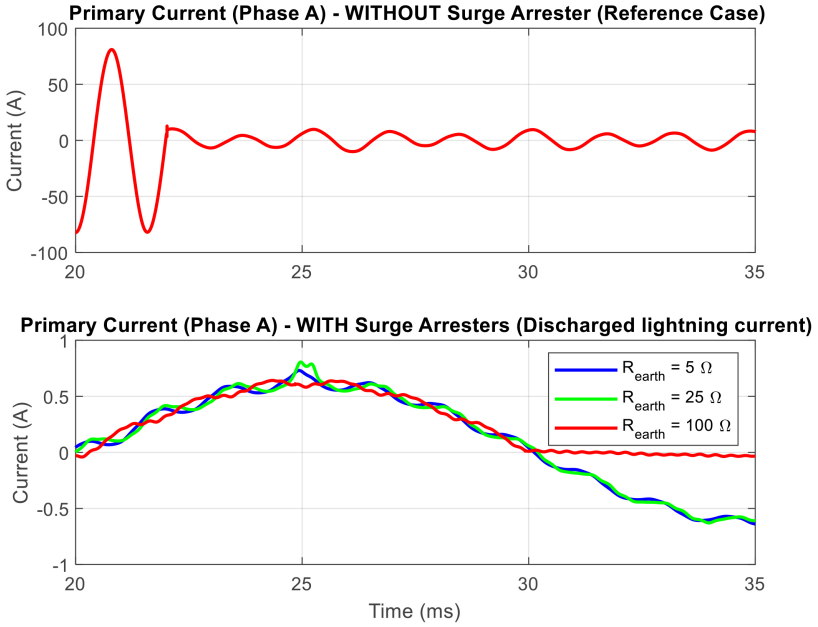


Figure 8. Primary-side transient currents.

Figure 8 shows that the short-circuit current reaches nearly 80 A with strong oscillations for the transformer without surge arresters. In the case of the transformer equipped with a surge arrester, the current peak is significantly attenuated, remaining around 0.8 A. The lightning current is instantly diverted to ground. The expanded observation window of 20 to 35 ms illustrates the impact of the

transient on the 50 Hz sinusoidal waveform.

3.1.3. Secondary-Side Transient Voltages

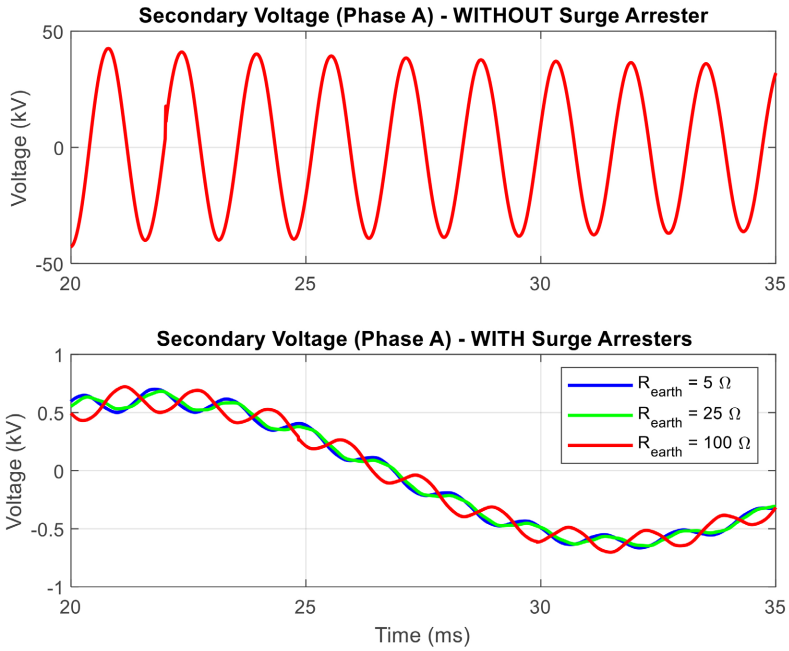


Figure 9. Transient voltages on the secondary side.

Figure 9 shows that on the secondary side of a transformer without surge arresters, capacitive and inductive coupling between the windings transfers a destructive overvoltage to the low-voltage side, reaching nearly 45 kV. This results in the immediate destruction of all downstream customer equipment or PV inverters. In contrast, on the secondary side of a transformer equipped with surge arresters, the transmitted voltage remains well below the 1 kV transient threshold, preserving the integrity of the LV infrastructure. The expanded observation window of 20 to 35 ms illustrates the impact of the transient on the 50 Hz sinusoidal waveform.

3.1.4. Secondary-Side Transient Currents

Figure 10 illustrates the behavior of the unprotected transformer, showing a secondary current peak reaching a critical value in the range of 2600 A to 2700 A at the moment of impact (inducing severe electrodynamic stresses on the windings). In contrast, with surge arresters installed, the line currents are smoothed and rapidly return to the grid's nominal dynamic state; the current peak is drastically reduced to approximately 24 A.

In both cases—without and with surge arresters—it is evident that the lightning current amplitude generates increasingly dangerous overvoltages (Figure 7 and Figure 9). The simulation results shown in Figure 8 and Figure 10 indicate that the lightning current amplitude affects the overvoltage distribution within the transformer substation. Furthermore, the results demonstrate that the surge arresters function correctly by reducing the voltages at the terminals of both trans-

formers. The dynamic behavior of the surge arresters must be taken into account to accurately predict terminal voltages across the substation's various pieces of equipment, particularly those with non-self-restoring insulation, such as transformers. The observation window, extended from 20 to 35 ms, illustrates the impact of the transient on the 50 Hz sinusoidal waveform.

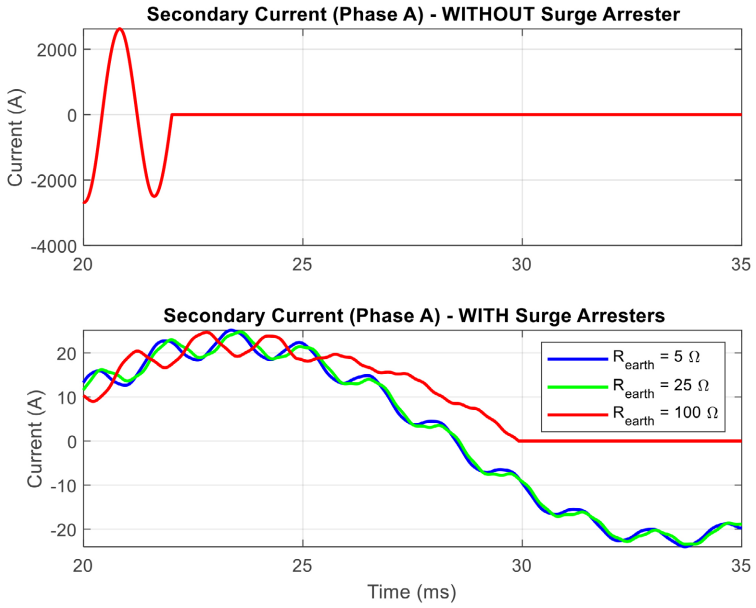


Figure 10. Secondary-side transient currents.

3.2. Protection Performance of ZnO Surge Arresters

3.2.1. Installation Distance for Protective Equipment

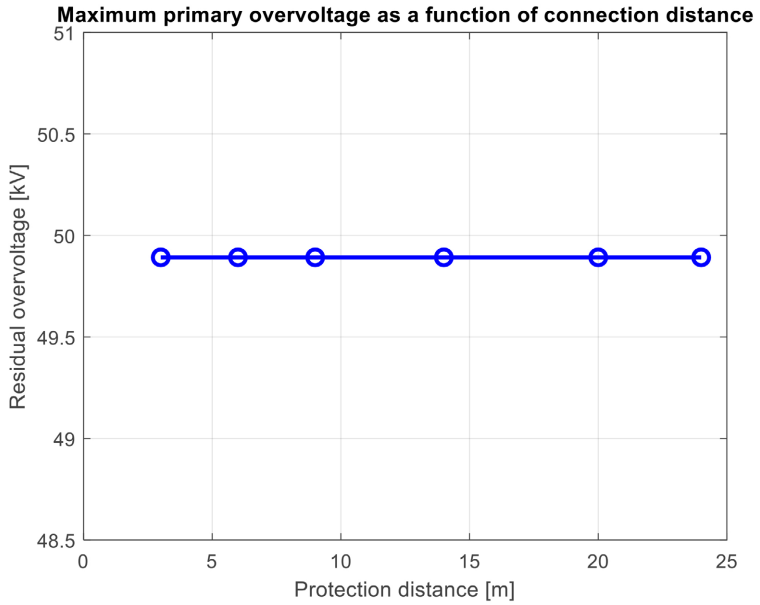


Figure 11. Variation of the maximum transient residual overvoltage (U_res) at the primary winding as a function of the ZnO surge arrester connection distance.

The length of the connecting cables refers to the length of the conductors connected to the surge arrester terminals (phase/neutral) and to the earth. This length must not exceed one meter (<1 m) to prevent overvoltage caused by wire inductance at the moment of sparkover. Indeed, surge arresters should be installed as close as possible to the transformers to effectively limit surge peaks to suitably low levels. While distance is irrelevant in an ideal connection model (assuming no connection inductance), in practice, conductor inductance necessitates placing the surge arrester as close as possible.

Figure 11 examines the effect of the connection distance, covering a protection distance range of 3 m to 24 m—representing the physical distance along the line between the surge arrester and the transformer. In this figure, the curve remains flat at 49.9 kV. This indicates that the simulated distance (3 m to 24 m) has no impact on the result within this model. This behavior confirms that the line separating the surge arrester from the transformer was modeled as an ideal connection—that is, one without impedance or propagation delay.

3.2.2. Sensitivity Analysis Regarding Lightning Strike Severity

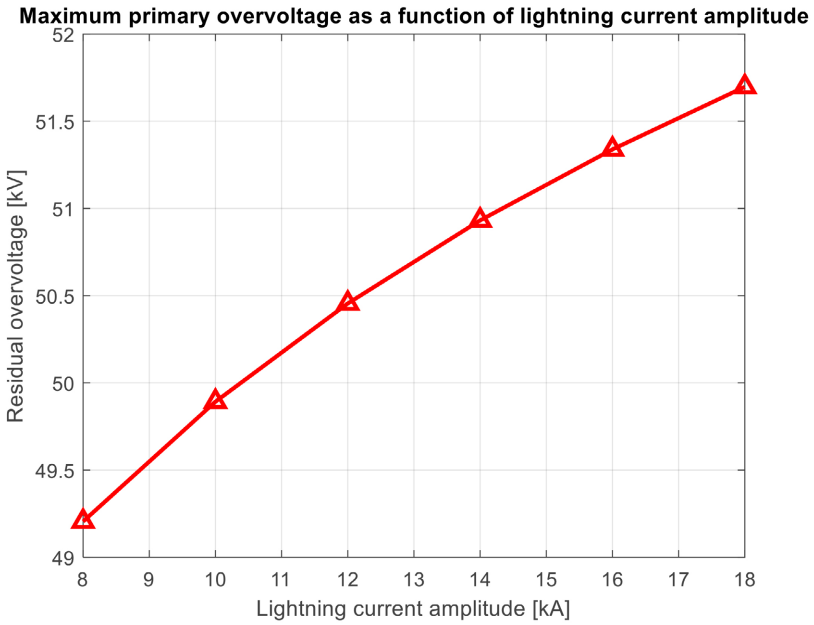


Figure 12. Sensitivity of the maximum transient residual overvoltage on the primary side to the amplitude of the injected lightning current.

Figure 12 examines the effect of lightning current amplitude—ranging from 8 kA to 18 kA—on the maximum stress experienced by the equipment. It reveals a clear, linearly increasing relationship: the residual overvoltage rises from approximately 49.2 kV for an 8 kA surge to nearly 51.7 kV for an 18 kA surge. The resulting overvoltage remains well below the typical Basic Insulation Level (BIL) of a 15 kV transformer, which is generally around 75 kV or 95 kV. The transformer under study is therefore fully protected against variations in amplitude.

This increase is directly linked to the non-linear static (V-I) characteristic of the surge arresters. Although they effectively clamp the voltage—reducing the thousands of kilovolts seen in the reference case to around 50 kV—their non-linear internal resistance causes a slight rise in terminal voltage as the discharge current intensifies.

3.2.3. Overvoltages Transmitted to the Secondary Side

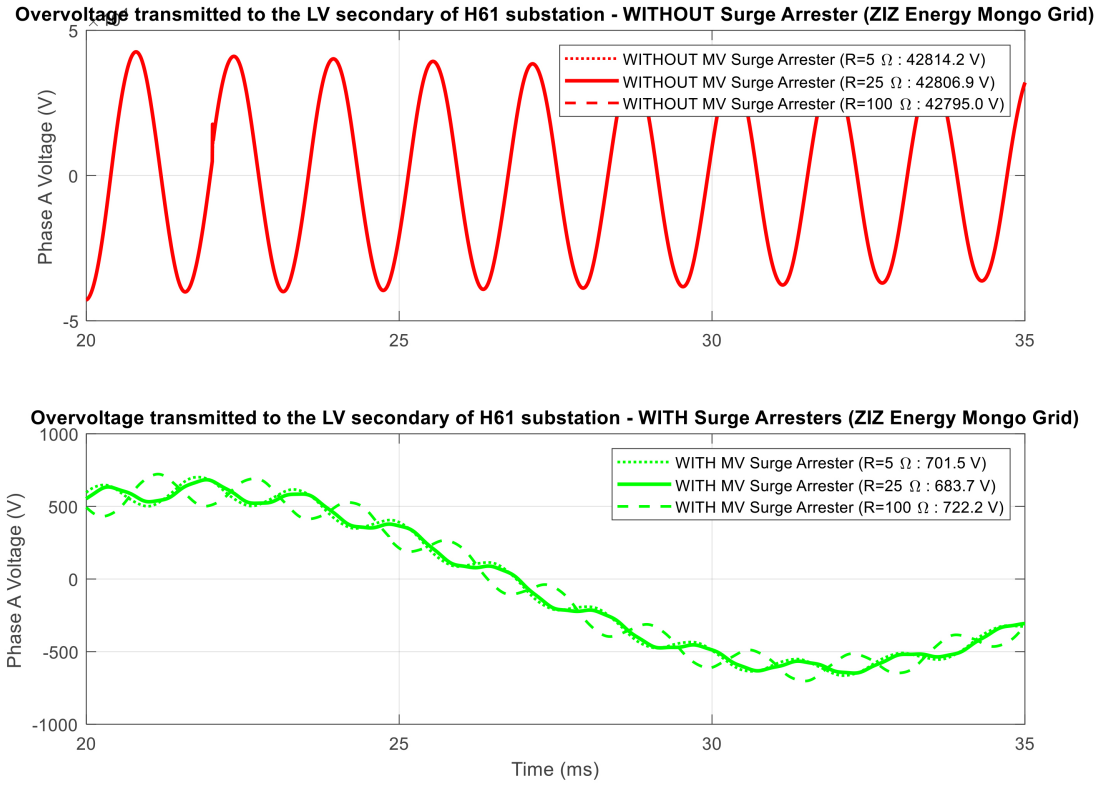


Figure 13. Overvoltages transmitted to the LV secondary of the H61 substation.

Figure 13 illustrates the phenomenon of overvoltage transfer from the primary (MV) to the secondary (LV) side of the H61 transformer. In the case of the transformer without an MV-side surge arrester, the dielectric surge passes through the transformer extensively via capacitive and inductive coupling. A destructive, oscillatory transient AC overvoltage is observed, reaching a critical peak of 42.8 kV, regardless of the earth resistance value (R_{earth} = 5, 25, or 100 Ω). With the MV-side surge arrester installed, the primary-side waveform is clipped, thereby suppressing the transferable energy. The secondary-side overvoltage is significantly damped, remaining within the range of 0.7015 kV (for 5 Ω earth resistance), 0.6837 kV (for 25 Ω), and 0.7222 kV (for 100 Ω). Although these levels exceed the 400 V nominal voltage, the attenuated transient value confirms the effectiveness of the filtering and demonstrates that a Type 2 LV-side surge arrester will suffice to eliminate the residual voltage and fully secure the power plant. The expanded observation window (20 to 35 ms) illustrates the impact of the transient on the 50

Hz sinusoidal waveform.

4. Conclusions

This study focused on analyzing and modeling the protection system for ZIZ Énergie's H61 substations in Mongo, located in the Sahel region, specifically during the rainy season.

It was found that, in the absence of surge arresters on the transformer's primary side, lightning strikes cause severe damage and can destroy the transformer. Voltage levels surge to theoretically destructive values of approximately 2500 kV. Such overvoltages impair the proper functioning of H61 substations and disrupt service continuity. Short-circuit current peaks at 80 A, accompanied by significant oscillations. By installing surge arresters—and ensuring they are placed as close as possible to the transformer—protection becomes effective and adequate. The overvoltage instantly drops below the 25 kV threshold—a perfectly tolerable level for ZIZ Énergie's 15 kV grid—and the lightning current is immediately diverted to the ground. On the transformer's secondary side, capacitive and inductive coupling between windings transfers a destructive overvoltage of up to 45 kV to the low-voltage circuit. This results in the immediate destruction of downstream customer equipment or PV inverters.

Regarding the influence of earth resistance: the higher the resistance, the more the transient pulse causes a local rise in ground potential. This voltage adds to the surge arrester's intrinsic residual voltage, thereby reducing the transformer's dielectric safety margin. Consequently, the installation of surge arresters is essential to mitigate atmospheric overvoltages in medium-voltage (MV) systems.

This study provides a robust decision-making tool that researchers and engineers can utilize to design an optimal protection system tailored to the seasonal conditions of the Sahel region. Research has focused on pole-mounted H61 distribution substations; however, future prospects for strengthening grid resilience suggest extending the study of protection against atmospheric overvoltages to all transformers at the power plant.

Author Contributions

Yacoub Nassian Nimir designed the study and defined its methodology. He also collected the data, performed the simulations, analyzed the results, and wrote the manuscript. Haroun Abba Laban participated in data collection and the interpretation of the results. Mahamat Wadi developed and programmed the computational tools and contributed to the validation of the results. Moussa Ahmat supervised the work and participated in the development of the methodology as well as the validation of the conclusions. All authors contributed to the interpretation of the data and reviewed, revised, and approved the final version of the manuscript.

Conflicts of Interest

The authors declare no conflicts of interest regarding the publication of this paper.

References

[1] Bedoui, S. and Bayadi, A. (2007) Atténuation des surtensions dans les postes de transformation haute tension par l'emploi des parafoudres ZnO. Université Ferhat Abbas. http://dspace.univ-setif.dz:8888/jspui/handle/123456789/9

[2] Forma TIS (2026) Parafoudre. Forma TIS. https://blog.formatis.pro/parafoudre/

[3] (2014) Surge Arresters—Part 4: Metal-Oxide Surge Arresters without Gaps for A.C. Systems. https://cdn.standards.iteh.ai/samples/18691/570872f782d245c8b028278532ab73a4/IEC-60099-4-2014.pdf

[4] Aoues, M.M., Birouche, M.C., Miouat, M.A. and Djoudi, M.H. (2014) Etude des protections d'un réseau MT application poste de boukhalfa 60/30kV. Université Mouloud Mammeri. https://dspace.ummto.dz/

[5] Safia, K. and Lila, B. (2011) Protection des transformateurs MT/BT contre les surtensions de foudre. Université Mouloud Mammeri. https://dspace.ummto.dz/handle/ummto/8531

[6] Bouzid, S. and Imarazene, A. (2014) Modernisation de la protection des autotransformateurs contre les surtensions atmosphériques. Mémoire de Master, Université Mouloud Mammeri de Tizi-Ouzou.

[7] Aoudia, M., Azzoug, A. and Belhocine, M. (2011) Etude des protections du poste source freha 60/30 kv contre les surtensions. Université Mouloud Mammeri de Tizi-Ouzou. https://dspace.ummto.dz/server/api/core/bitstreams/ee5361b5-e683-4e33-8cae-a2116308681d/content

[8] INSEED (2026) Institut national de la statistique et des études économiques et demographiques. INSEED. https://www.inseed.td/

[9] Studocu (1996) NF C 11 201: Réseaux de distribution publique d'énergie. https://www.studocu.com/row/document/universite-de-ndjamena/exercice-pratique/nf-c-11-201-reseaux-de-distribution-publique-denergie-norme-1996/148935577

[10] Parafoudres. https://assets.legrand.com/general/ouidoo/pdf/legrand-guide-technique-parafoudres.pdf

[11] Shutterstock (2026) 1,3 Millier Images et Photos de Lightning over Beach Libres de Droits. https://www.shutterstock.com/fr/search/lightning-over-beach

[12] IEEE Standards Association (2026) IEEE Standard for Metal-Oxide Surge Arresters for AC Power Circuits (> 1 kV). https://standards.ieee.org/ieee/C62.11/5839/

[13] Bayadi, A., Harid, N., Zehar, K. and Belkhiat, S. (2003) Simulation of Metal Oxide Surge Arrester Dynamic Behavior under Fast Transients. *Proceedings of the International Conference on Power Systems Transients* (*IPST*), New Orleans, June 2003.

[14] Meghezzi, A. and Sidi Said, A. (2013) Étude des surtensions dues à la ferrorésonance en phases incomplètes. https://dspace.ummto.dz/server/api/core/bitstreams/36ea55f0-b4f7-423c-8179-fad57d0c5845/content

[15] 30kV/BT 160kVA-100kVA-50kVA MT transformateurs haut de poteau huile de type H61_fabricant de Chine-Engelec Power Technology CO., LTD. https://www.engelecgroup.com/30kV-BT-160kVA-100kVA-50kVA-MT-transformateurs-haut-de-poteau-huile-de-type-H61-pd767411198.html

[16] Mahseredjian, J., Xémard, A. and Khodabakhchian, B. (2007) Régimes transitoires dans les réseaux électriques. https://www.techniques-ingenieur.fr/ressources-documentaires/energies-th4/conversion-de-l-energie-electrique-ti301/regimes-transitoires-dans-les-reseaux-electriques-d82

List of Abbreviations

ANSI: American National Standards Institute
MV: Medium Voltage
LV: Low Voltage
ZIZ: Zakharia Ibrahim Zakharia
PV: Photovoltaic
MATLAB: MATrix LABoratory
CT: Current Transformer
VT: Voltage Transformer
RCD: Residual Current Device
IEC: International Electrotechnical Commission
PT: Potential Transformer
HRC: High Rupturing Capacity
HV: High Voltage
AM: Air Mass
DC: Direct Current
AC: Alternating Current
RMS: Root Mean Square
BIL: Basic Impulse Insulation Level (or sometimes Basic Insulation Level)
RLC: Resistance, Inductance, Capacitance
RS: Reset-Set